Comparison of Chest Radiographs with Minimum Intensity Projection Reconstruction CT Scans for the Presence of Airway Stenosis Resulting from Lymphobronchial TB in Children

Dr Dewald Bester

A research report submitted to the Faculty of Health Sciences, University of the Witwatersrand, Johannesburg, in partial fulfilment of the requirements for the degree of Master of Medicine in Radiology

Johannesburg, 2021

Declaration

I, Dewald Bester, declare that this research report is my own work. It is being submitted for the degree of MMed (RadD) at the University of the Witwatersrand, Johannesburg. It has not been submitted before for any degree or examination at this or any other University.

DR DEWALD BESTER

On this 26th day of February 2021

I dedicate this thesis to:

My amazing wife Rita your love and support guided and strengthened me through many challenges.

Publications and presentations

This work has never been published.

It has never been presented at a congress.

Abstract

INTRODUCTION:

The diagnosis of tuberculosis (TB), and in particular lymphobronchial tuberculosis (LBTB), in children continues to rely on imaging. Modern computed tomography (CT) imaging with coronal minimum intensity projection (MinIP) reconstruction is ideally suited for diagnosing airway compression in LBTB. Resource constraints in developing countries, however, oblige medical practitioners to use plain radiography in the evaluation of children with LBTB. Identification of airway compression on chest X-ray (CXR) is important, as it may be the only diagnostic feature of TB for instituting treatment.

AIM:

The aim of this study was to demonstrate the sensitivity and specificity of frontal CXR in identifying airway stenosis, at ten specific sites, against the gold standard, CT MinIP and to determine the agreement between the modalities regarding the degree of stenosis.

METHOD:

This was a retrospective, quantitative cross sectional study comparing CXR and CT MinIP in 37 children with confirmed LBTB at 10 predetermined airway locations.
The CXRs were evaluated by one expert reader a paediatric radiologist, the CT MinIP images were evaluated by three general radiologists

RESULTS:

Patients age ranged from 2months 22 days to 147 months 25 days. The median age of the patients was 14.3 months (interquartile range 8.0-23.2 months; range 2.7-147.8 months). The original database of patients included a total number of 212 patients, of which only 41 had a CXR available. Of those 41 patients only 37 had a CT MinIP and 4 did not, thus the final study population was 37 in total. Chest X-ray demonstrated that 31 out of the 37 patients in the study group thus 84%, had stenosis at least at one of the ten evaluated sites, confirmed on the CT MinIP images. Computed tomography MinIP, which is taken as the gold standard, showed that all 37 patients, thus 100%, had stenosis at one of the ten evaluated sites.

The sensitivity for CXR picking up stenosis at the left main bronchus (LMB) was 92.9%, with a 100% specificity.
The sensitivity for stenosis at the bronchus intermedius (BI) was 80% with a specificity of 75%.
The kappa agreement between CXR and Minip with regard to the grade of stenosis for each site shows substantial agreement (Kappa 0.67) for the LMB and moderate agreement (kappa 0.58) for the BI.

CONCLUSIONS:
In a paediatric population where the incidence and the severity of airway stenosis from LBTB is high, CXR was shown to be accurate in detecting airway stenosis and in demonstrating severe stenosis at the LMB and BI.

Acknowledgements

1) Prof Savvas Andronikou my primary supervisor, for assisting me throughout with creative solutions and ideas, for co-reading the CXR and CT MinIP images and for your help with the final drafts and thesis completion.
2) Dr Susan Lucas my secondary supervisor, for all the teaching and guidance along the way, and all your help with the final drafts and completion of my thesis.
3) Prof V. Mngomezulu for granting me research time to complete the thesis.
4) Dr Pierre Goussard and Professor Robert Gie of the department of Paediatrics, Stellenbosch University for the permission to use their database.
5) Dr Ahmed Krim for co-reading the radiographs and CT MinIP images.
6) Dr Petra Gaylard from the DMSA for all your help with the statistical analysis.
7) Mrs Noleen Gordon for assisting with the Microsoft Word and Excel challenges.
8) My wife Rita for your encouragement throughout this thesis and the years specialising.

Table of Contents

Declaration ii
Publications and presentations iv
Abstract v
Acknowledgements vii
Table of Contents viii
List of Figures x
List of Abbreviations and Terminology xii
1. Introduction 1
1.1. Epidemiology of TB 1
1.2. Impact of HIV on TB 2
1.3. Pathogenesis of TB in children 2
1.4. Laboratory tests to confirm TB 3
1.5. Imaging techniques 3
1.5.1. Chest Radiograph 4
1.5.2. CT scan of the Chest 4
1.5.3. Other imaging techniques 4
1.6. Chest radiograph findings in TB and LBTB 5
1.7. CT findings in TB and LBTB 6
1.8. Diagnostic workup for airway compression 6
1.9. Rationale and summary 7
1.10. Aim
1.11. Objectives ..... **Error! Bookmark not defined.**
2. Materials and Methods 9
2.1. Parent study
2.2. Inclusion and exclusion criteria 9
2.2.1. Inclusion Criteria 9
2.2.2. Exclusion Criteria 10
2.3. Data collection 10
2.3.1 Radiology reading procedures 10
2.4. Statistical analysis 14
2.5. Ethics 14

3. Results 15
3.1. Demographics 15
3.2. Presence of airway stenosis by site 16
3.3. Severity of stenosis on CXR and MinIP 18
3.3.1. By site 18
3.3.2. Overall number of stenoses according to severity for CXR and CT MinIP 24
3.3.3. Number of patients who demonstrated stenosis in any of the ten predetermined sites 24
4. Discussion 25
4.1. Limitations of the current study 29
4.2. Current applications 29
4.3. Future applications 29
5. Conclusion 31
6. References 32
Appendix A: Ethics Clearance Certificate 36
Appendix B: Permission letter from Prof P. Goussard
Appendix C: Tick sheet site and degree of airway narrowing on CXR 38
Appendix D: Tick sheet site and degree of airway narrowing on CT MinIP 39
Appendix E: Note on referencing style 40

List of Figures

Figure 2.1. Examples of paediatric airway stenosis in patients with LBTB demonstrated on CXR and CT MinIP ..... **Error! Bookmark not defined.**

Figure 3.1. Flow diagram demonstrating the derivation of included patients ..... **Error! Bookmark not defined.**

Figure 3.2. Age of patients..... **Error! Bookmark not defined.**

Figure 3.3. Percentage of stenosis by site as determined by CXR and CT MinIP ..... **Error! Bookmark not defined.**

Figure 3.4. Grading of stenosis on CXR..... **Error! Bookmark not defined.**

Figure 3.5. Grading of stenosis on CT..... **Error! Bookmark not defined.**

List of Tables

Table 3.1. Percentage of patients with stenosis diagnosed by each modality ..... **Error! Bookmark not defined.**

Table 3.2. Estimation of the sensitivity and specificity of CXR for the detection of stenosis with regards to CT MinIP for each site ..... **Error! Bookmark not defined.**

Table 3.3. Percentage of severe stenosis per site according to CXR evaluation..... **Error! Bookmark not defined.**

Table 3.4. Percentage of severe stenosis per site according to CT MinIP evaluation.. **Error! Bookmark not defined.**

Table 3.5. Agreement between CXR and CT with regards to the grade of obstruction for each site..... **Error! Bookmark not defined.**

Table 3.6. Overall number of stenosis according to severity for CXR and CT MinIP..... **Error! Bookmark not defined.**

List of Abbreviations and Terminology

A:	AIDS	acquired immune deficiency syndrome
	AP	antero-posterior
B:	BI	bronchus intermedius
C:	CT	computed tomography
	CXR	chest X-ray
D:	DICOM	digital imaging and communications in medicine
E:		
F:	FTB	fibreoptic tracheobronchoscopy
G:		
H:	HIV	human immunodeficiency virus
I:	IV	intravenous
J:		
K:	kV	kilovolt
	Kg	kilogram
	K	kappa
L:	LBTB	lymphobronchial tuberculosis
	LMB	left main bronchus
	LULB	left upper lobe bronchus
	LLLB	left lower lobe bronchus
M:	MinIP	minimum intensity projection
	M. tuberculosis	*Mycobacterium tuberculosis*
	MRI	magnetic resonance imaging
	mAs	milliampere-second
	MIP	maximum intensity projection
	MPR	multiplanar reformatting

	ml	millilitre
	MDCT	multidetector computed tomography
N:	N	normal diameter of the airway
	n	number of patients/sample size
O:		
P:	PCR	polymerase chain reaction
Q:		
R:	RMB	right main bronchus
	RULB	right upper lobe bronchus
	RMLB	right middle lobe bronchus
	RLLB	right lower lobe bronchus
S:	SSD	shaded surface display
	S	minimum diameter of airway at level of stenosis
T:	TB	tuberculosis
U:	US	ultrasound
V:	VR	volume rendering
W:	WHO	World Health Organisation
X:		
Y:		
Z:		

1. Introduction

Tuberculosis is a bacterial disease which is caused through infection with *Mycobacterium tuberculosis (M. tuberculosis)* (1). Lymphobronchial tuberculosis is a described entity by which enlarged lymph nodes cause airway obstruction and related severe complications involving the lung parenchyma.

The diagnosis of TB, and in particular LBTB, in children continues to rely on imaging. Modern CT imaging with MinIP reconstruction is ideally suited for diagnosing airway compression in LBTB. Resource constraints in developing countries, however, oblige medical practitioners to use plain radiography in the evaluation of children with LBTB. Identification of airway compression on CXR is important, as it may be the only diagnostic feature of TB for instituting treatment.

1.1. Epidemiology of TB

Tuberculosis is a major cause of mortality and morbidity globally and almost a third of the population worldwide is affected (2, 3). Approximately 2-3 billion individuals are infected with *M. tuberculosis* globally, however only a small percentage ranging from 5-15% will develop TB disease (4). Human Immunodeficiency Virus (HIV) infection raises the probability of developing TB disease (4). The global TB report for 2016 compiled by the World Health Organization (WHO), shows that the best assessment for 2015 is that globally there were 10.4 million new TB cases, out of which 1.0 million were related to children, 5.9 million were amongst men, 3.5 million among women. This figure of 10.4 million included the 1.2 million among HIV-infected individuals (4). According to the report, TB now ranks above HIV/AIDS as a principal cause of mortality due to an infectious disease, and is amongst the ten primary causes of global deaths (4). The report states that 1.4 million mortalities resulting from TB worldwide occurred in HIV non-reactive individuals during 2015 and a further 0.4 million deaths resulted from TB disease among HIV infected people (4). Tuberculosis affects all age groups from infants to the elderly (5), the distribution of incident cases in 2015 were 90% adults and 10% children (4) worldwide.

The lowest TB rates are found mainly in high-income nations including most countries in Western Europe, the United States of America, Canada, Japan, Australia and New Zealand. The incidence rate of TB in these countries is less than ten cases per 100 000 population (6). The following nations account for 60% of new TB cases: India, Indonesia, China, Nigeria, Pakistan and South Africa (4). India has emerged in the interim as the nation with the highest incidence of TB disease in the world after estimates for the period 2000-2015 were revised upwards (4). The incidence rate of new TB cases in 2015 was above 500 per 100 000 population in South Africa, Lesotho and Mozambique (4). In the WHO African Region the percentage of TB cases co-infected with HIV was the largest and in parts of South Africa surpassed 50% (4). According to the District Health Barometer report 2015/16 the provinces with the highest incidence rates of tuberculosis in South Africa are the Eastern Cape (692), KwaZulu-Natal (685) and Western Cape (681) per 100 000 population (7).

1.2. Impact of HIV on TB

Mycobacterium tuberculosis causes infection in one third of the world's population but in most people it remains latent unless HIV or other factors weakens the immune system, which then leads to clinical disease. A patient who has latent TB infection has a 10% chance of developing active disease each year, if infected with HIV (8).

1.3. Pathogenesis of TB in children

Inhalation of *M. tuberculosis* bacilli is the most frequent mode of infection with the pathogen lodging in a terminal airway or alveoli causing a localized lung response described as the primary parenchymal or Ghon focus (9). Tuberculosis bacilli drain away from this focus through the local lymphatic pathways to the regional lymph nodes (9) with large hilar and mediastinal nodes being the hallmark of initial TB infection (10). When the airways are involved by *M. tuberculosis* infected lymph nodes, LBTB is the result (11). The lymph nodes compress the adjacent regional bronchi and cause bronchial wall inflammation (10). Airway obstruction in paediatric patients is aided by the small diameter of the airways and the lack of rigidity, making them prone to compression (12).

1.4. Laboratory tests to confirm TB

The diagnosis of TB is often inaccurate and difficult with less than 40 % of the cases being confirmed (13). Bacteriological confirmation, the accepted gold standard, is of limited use in children due to the low numbers of bacilli and due to the low bacteriological turnover (14), it is reported that *M. tuberculosis* is isolated in less than 30 – 40 % of children (15). Specific tests that are used include sputum smear microscopy (positive diagnostic yield in less than 10 – 15%) and sputum culture (30-40% positive yield in children with probable TB. These tests also have limitations including the fact that small children have difficulty in expectorating sputum (16). Nasopharyngeal aspirates, gastric lavage and bronchoalveolar lavage are therefore used in young children who cannot produce sputum (14).

A positive tuberculin skin test indicates that a child has been exposed to the bacillus, but has the following limitations: TST cannot distinguish between active and latent infection (17) and is often positive in healthy children from endemic areas (14). TST cross-reacts with BCG vaccine, has a poor TB detection rate in HIV infected children and less than 50% of bacteriologically proven TB cases have a positive TST test result (14). TST is inaccurate in children with severe malnutrition, micronutrient deficiencies or other viral infections such as measles. Often patients do not return two to three days later for analysis of the results (18).

Other types of specimens that are investigated include fine-needle lymph node aspirates, bone marrow , urine, stool and sterile fluid such as cerebrospinal, ascitic and pleural fluid. All the above mentioned specimens are low in yielding bacilli except for lymph nodes and bone marrow (18). Other tests used to diagnose infection with *M. tuberculosis* include the culture of infected material, nucleic acid amplification test for TB called Xpert (sensitivity 74.3% in children) and loop mediated isothermal amplification assay (sensitivity 88-100%, specificity 94-99% in sputum) (18).

1.5. Imaging techniques

The basis of the radiological diagnosis of primary TB disease in paediatric patients is the detection of perihilar and paratracheal lymphadenopathy (9). Lymphadenopathy can however be caused by a variety of other non-infective conditions including mediastinal malignancies of lymphatic, thymic, neurogenic, germ cell and mesenchymal origin of which lymphoma is the most common (19). Further causes of mediastinal lymphadenopathy

include: Langerhans Cell Histiocytosis, a clonal neoplastic proliferation of Langerhans cells normally found in lymphatic, thymic, lung and skin tissue (20), granulomatous diseases such as Sarcoidosis (21) and proliferation of non-neoplastic histiocytes in lymphnode sinuses as seen in Rosai Dorfman disease (22) amongst others. In view of these other entities it is important to review the chest radiograph findings in conjunction with other parameters to make the correct diagnosis: In non-endemic areas the diagnosis of TB is made on a history of contact with an adult TB case, a positive TST and positive findings on the chest radiograph (14). In endemic areas the diagnosis is made on the presenting clinical features and interpretation of the chest radiograph (14, 16, 23).

1.5.1. Chest radiograph

In children this investigation in the form of anteroposterior (AP) and lateral CXR combination is the first and the most frequently used radiological modality (1). However, only approximately 60 % of paediatric patients with a normal CXR will demonstrate lymphadenopathy on a chest CT (24), thus CXR is insensitive for the detection of lymphadenopathy (13, 24). It is however accurate in depicting airspace disease, the Ghon focus, interstitial disease and pleural effusions (13).

1.5.2. CT scan of the chest

CT has an advantage over CXR because it confirms the presence of lymphadenopathy, delineates the degree of the infective process and the various associated complications (1, 25). CT post processing techniques allow for a greater quantity of scan information to be evaluated thus making it more effective in making a precise diagnosis, especially in the paediatric population (26). CT is commonly used for disseminated, complicated and unusual forms of TB (1).

1.5.3. Other imaging techniques

Magnetic resonance imaging (MRI) (1) and ultrasound (US) of the chest (1, 27, 28) can both demonstrate mediastinal lymphadenopathy. Amongst the limitations of MRI is the need for sedation or general anaesthesia with respiratory gating (13) which in turn may present its own risks. There may also be restricted accessibility in countries where TB is highly prevalent (13). High cost involved and inadequate demonstration of the lung tissue are the other disadvantages (1).

The advantages of US include it being a low cost modality, the patient is not subjected to radiation, the lesion or area of interest can be evaluated from many different angles and the examination entails uncomplicated handling of the probe, thus the technique is easily learnt. Short procedure time provides the ability to do multiple repeat examinations as well as the ability to evaluate majorly sick patients at the bedside. US has the advantage of evaluating pathology or doing biopsies in real time, determining precisely what structures are being traversed or sampled (28) The disadvantages of US include being very operator dependent (28, 29) and that this imaging method may not demonstrate deep mediastinal (29) or deep parenchymal (28) pathology.

1.6. Chest radiograph findings in TB and LBTB

The most prevalent finding occurring in over 90% of children with primary TB is hilar and mediastinal lymphadenopathy (30). The anteroposterior radiograph demonstrates lymph node enlargement as a sharply or poorly defined lobulated radiopacity involving the hilum with a loss of the normal sharp hilar point (13). The lateral projection is used to demonstrate lymphadenopathy posterior and inferior to the BI (31); these enlarged nodes complete the lower portion of a doughnut shaped density, the upper portion of the doughnut being formed by the right and the left pulmonary arteries and the aortic arch (13). Although rare, calcification in lymph nodes and the parenchymal focus can occur and correspond to a healed lesion (31). Air space parenchymal disease (consolidation) which appears as merging areas of radiodensity with air bronchograms and round or oval parenchymal lesions representing tuberculomas or parenchymal nodules may be identified but are found in many other infections and non-infectious pathologies. Miliary nodules, cavitation, fibrosis and scarring as well as pleural effusions may occur (31).

The primary finding of LBTB is airway compression by lymphadenopathy. Airway compression commonly affects the right main bronchus (RMB) and BI (32-34) with associated lung collapse consolidation as seen on CXR and CT, most frequently affecting the right lung (34). Alternatively the bronchial narrowing in LBTB may cause obstructive hyperinflation (30, 31).

1.7. CT findings in TB and LBTB

On post contrast CT studies, the "rim sign" is typical of TB lymphadenopathy and consists of a lymph node with a hypodense necrotic centre and an enhancing rim of tissue (31). Consolidation, parenchymal nodules, a miliary pattern, cavitation, scarring and fibrosis as well as effusions can be identified (31). Findings more specifically associated with LBTB include enlarged lymph nodes causing airway compression and complicated by hyperinflation, consolidation, wet lung, necrosis, bulging fissures and eventual calcification in lymph nodes (24, 31, 35).

1.8. Diagnostic workup for airway compression

Chest X-ray, CT and fibre-optic tracheobronchoscopy (FTB) are used to diagnose airway obstruction in children (24). Fibre-optic tracheobronchoscopy demonstrates intraluminal narrowing, external compression and the degree of stenosis (24). Other advantages of FTB include the technique being relatively safe to perform, the ability to enucleate enlarged lymphnodes, aspiration of endobronchial contents and transbronchial biopsy (24, 26). Fibre-optic tracheobronchoscopy is limited in that it does not demonstrate the cause of stenosis and because it is unable to demonstrate the relation between the thoracic vessels and airway stenosis. Airways, which are not easily accessed, and those beyond a tight stenosis, are difficult to navigate with FTB. Fibre-optic tracheobronchoscopy also has the disadvantage that it requires general anaesthesia which can result in complications, and is an invasive procedure (24).

Due to these reasons, CT with various post processing techniques is a useful alternative as they are easily performed and due to the speed of the imaging no form of anaesthesia is needed. The disadvantage of CT is that the child is exposed to radiation but this can be minimised by reducing the kilovolt (kV) and milliampere-second (mAs); the radiation dose can be decreased by up to 65% (24). Computed tomography post processing techniques allow for a greater quantity of scan information to be evaluated at the same time thus making it more effective in making a precise diagnosis especially in the paediatric population (26). The post processing techniques in use include: MinIP, maximum intensity projection (MIP), multiplanar reformation (MPR), shaded surface display (SSD) and volume rendering (VR) (26). Minimum intensity projection demonstrates low density structures such as the large airways (36, 37) and is ideally suited for enhancing the study of paediatric airways (38).

Minimum intensity projection works in the following way: A ray is cast ninety degrees to the coronal view through a selected thickness volume of data (the slab); the pixels with the lowest Hounsfield unit in this slab are used to create multiplanar slab images (26). By projecting the pixels with the lowest values the air filled structures such as the bronchial airways are accentuated against a homogenous background. An advantage of this method is that structures that have a 3D configuration such as the tracheobronchial tree can be evaluated in full length within a slab of tissue, thus making it possible to visualise the extent of a stricture in a single image (26). The pitfalls of thick slab MinIP is that the airway may not be included in the slab or that the orientation of the coronal plane reconstruction may cause cut off of the airway, but these can be mitigated against.

1.9. Rationale and summary

Lymphobronchial tuberculosis is a described entity by which enlarged lymph nodes causes airway obstruction and causes severe complications involving the lung parenchyma. Tuberculosis and in particular LBTB continue to rely on imaging tools for diagnosis and in particular modern CT imaging with coronal MinIP reconstruction is ideally suited for diagnosing airway compression in LBTB. Resource constraints in developing countries oblige medical practitioners to continue to use plain radiography in the evaluation of children with lymphobronchial TB instead of the more advanced CT reconstruction techniques. In addition identification of airway distortion and compression may be the only diagnostic feature of TB on plain radiographs for instituting treatment. No previous studies have compared the visualization of airway compression of LBTB on chest Xray with a CT gold standard to determine its usefulness. This study will use coronal MinIP as a gold standard for directly comparing a 2D frontal chest radiographs against.

1.10. Aim

The aim of this study is to prove that CXR which is a low cost and easily available modality can be sensitive and specific for detecting airway stenosis as a surrogate for lymphadenopathy in diagnosing TB in children, in a resource constrained environment.

1.11. Objectives

- Primary objective: To determine the detection rate of airway compression due to LBTB on CXR and to compare these findings to CT MinIP as gold standard, in order to establish the sensitivity and specificity of CXR in determining the site of compression
- Secondary objective: To determine the agreement between CXR and CT MinIP with regards to the degree of obstruction at these sites.

2. Materials and Methods

The current study was a retrospective, quantitative cross sectional study using a CT scan database of paediatric patients with LBTB who were imaged over the course of ten years at the Tygerberg Hospital Paediatric Pulmonology department in the Western Cape of South Africa. Patients presented with characteristics of severe airway stenosis and were placed on quadruple TB drug treatment with steroids added. After 30 days if there were still symptoms and radiological features of severe airway stenosis FTB and MDCT were performed 10 days apart. The current study was performed at the University of the Witwatersrand in Johannesburg South Africa in the Department of Diagnostic Radiology.

2.1. Parent study

The parent study was a prospective study done by Goussard et al over the course of ten years at the Tygerberg Hospital Paediatric Pulmonology department in the Western Cape of South Africa evaluating children with LBTB with FTB and CT scan.

One component of the parent study was published in Pediatric Radiology (2009) 39:694-702: Comparing three-dimensional volume-rendered CT images with FTB in the evaluation of airway compression caused by tuberculous lymphadenopathy in children. The study found 87 sites of airway stenosis on FTB, 138 sites of stenosis employing the three dimensional volume rendering (3-D VR) technique of which 78 sites (90%) matched the stenotic sites shown by FTB. The sensitivity and specificity of 3-D VR was shown as 92% and 85% when compared to FTB (24).

2.2. Inclusion and exclusion criteria

2.2.1. Inclusion criteria for parent study

- Children under 13 years of age
- Children who had a confirmed positive diagnosis of TB by means of culture or detection of acid-fast bacilli in gastric and pulmonary aspirates.
- Children with clinical signs and symptoms of large airway narrowing.
- Children who had persistent symptoms of upper airway obstruction after 30 days of anti-TB treatment combined with steroids.
- Known HIV status as determined by Polymerase Chain Reaction (PCR).

- Children who underwent FTB and CT of the chest as part of the routine diagnostic work-up.

2.2.2. Exclusion Criteria for current study

- Patients with incomplete data
- Cases where MinIP reconstructed images were not available
- Patients with a frontal CXR of inadequate quality or those in which the frontal CXR data was corrupt were excluded.

2.3. Data collection

An established database for a more extensive clinical project (the parent study) was used for a retrospective analysis of imaging studies.

Frontal chest radiographs were performed with a variety of digital X-ray radiographic equipment and CTs of the chest were performed on a 4 slice multidetector CT scanner (Aquilion, Toshiba, Nasu, Japan). A standard paediatric chest protocol was used with a 120 kVP tube voltage and 50 mA tube current. Intravenous iodinated contrast medium (low osmolar, non-ionic, 300 mg/ml iodine content) was injected by hand at a dose of +/-2 ml/kg body weight. The time delay between contrast injection and the acquisition of the images ranged from 30 – 35 seconds.

2.3.1 Radiology reading procedures

The original MDCT imaging data obtained was reconstructed by using a CT MinIP post processing technique to obtain coronal MinIP images which were directly compared to the frontal CXR. The coronal MinIP reconstruction was performed in a standardized way on an OsiriX DICOM Viewer 32.bit (version 5.6) software package using a standardised protocol with fixed slab thickness and angulation. These MinIP images were interpreted by 3 readers blinded to each other: Dr DB, Dr AK, both general diagnostic radiologists, and Dr SA, an experienced paediatric radiologist. The consensus majority decision (two or more for the presence of stenosis) results from all three readers CT MinIP findings were thus available and also used in this study. CXR interpretation of Dr SA (an experienced paediatric radiologist) was considered the expert reader interpretation of the frontal CXR

interpretations (performed in a separate sitting some months apart from the CT reading and blinded to the CT scans at the time of CXR interpretation). The frontal radiographs were interpreted by all three readers separately, the interpretations of SA were however used as those of the expert reader as most sites had low interrater agreement, significant interrater bias or were not commented on due to technical factors degrading the quality of the radiograph, resulting in poor visualization of the airway. The results from Dr SA were then compared to the consensus majority CT MinIP results.

The study group consisted of 37 patients, and the degree of airway stenosis at 11 predetermined sites along the tracheobronchial tree on frontal CXR and MinIP was determined and recorded in the data collection sheet (Appendix B and C). The sites evaluated were the: Trachea, Carina, RMB, Right upper lobe bronchus (RULB), BI, Right middle lobe bronchus (RMLB), Right lower lobe bronchus (RLLB), LMB, Left upper lobe brochus (LULB) and Left lower lobe bronchus (LLLB).

Numeric measurements were taken of all affected regions at the site of the most severe stenosis for each segment evaluated. The data was converted into a percentage by using the following formula:

$$\% \text{ Stenosis} = [1 - (S/N)] \times 100$$

Where S = Minimum diameter of the airway at level of stenosis

N = normal diameter of the airway, as measured proximal to the stenosis where the airway diameter was perceived to be normal

Obstruction at the different sites were categorised as follows:

- No obstruction 0% - Grade 0
- Mild obstruction 1-50 % - Grade 1
- Moderate obstruction 51-75% - Grade 2
- Severe obstruction 76-99% - Grade 3(a)
- Complete obstruction 100% - Grade 3(b)

This grading is based on the classification method used by Goussard et al in their 2012 study using FTB to determine airway stenosis (39). Severe stenosis was taken as grade 3a and 3b.

The percentage of severe stenosis at a site was calculated as follows: Percentage severe stenosis at site = severe stenosis at site (3a + 3b) ÷ total number of stenoses (all grades and sites).

Examples of airway stenosis found during this study are demonstrated in figure 2.1.

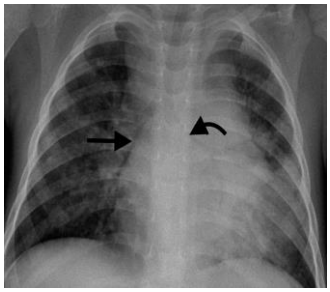

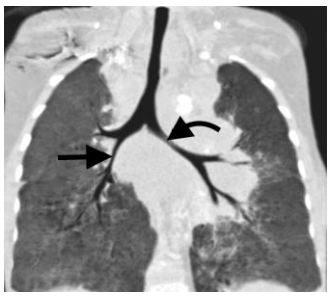

A. CXR and CT MinIP images of a 2year 8month old boy demonstrating BI stenosis (straight arrow) and LMB stenosis (curved arrow).

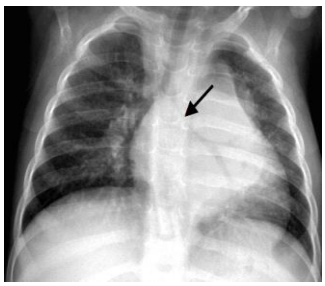

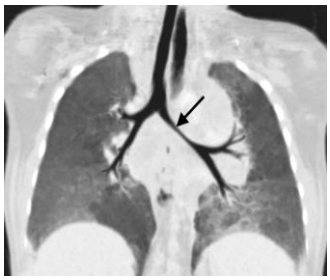

B. CXR and CT MinIP images of a 1year 11month old girl demonstrating LMB stenosis (straight arrow).

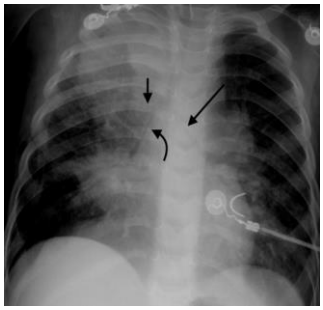

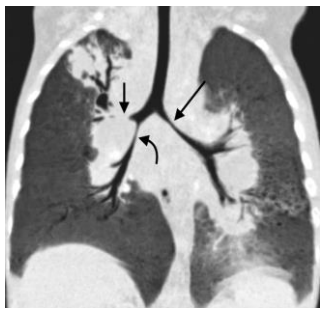

C. CXR and CT MinIP images of a 1year 11month old boy demonstrating LMB stenosis (long straight arrow), BI stenosis (curved arrow) and cut-off of the RUL bronchus (short straight arrow).

Note: RULB = right upper lobe bronchus, BI = bronchus intermedius, LMB = left middle lobe bronchus

Figure 2.1. Examples of paediatric airway stenosis in patients with LBTB demonstrated on CXR and CT MinIP

2.4. Statistical analysis

The CXR findings of SA were compared to the majority decision CT MinIP results.

Comparative statistics of agreement was applied to the following aspects:

a) Presence of stenosis at each site

b) Degree of stenosis at each site

For the percentage stenosis categories we used the Chi - square test.

Cross tabulation was used to delineate the categorical data and diagnostic tests including sensitivity, specificity, positive predictive value, negative predictive value and likelihood ratio was used against the reference standard CT MinIP reconstructed images.

Agreement between CXR and CT with regards to the grade of obstruction for each site was determined with the weighted kappa coefficient.

All the data collected were analysed using STATISTICA 9.1, a statistical software package by StatSoft, Inc. All statistical calculations were performed by Dr Petra Gaylard at the Data Management and Statistical analysis institute at the University of the Witwatersrand.

2.5. Ethics

The study was accepted by the Human Research Ethics Committee of the University of the Witwatersrand, approval number M140476. This certificate is attached as Appendix A.

Permission was obtained from Prof Pierre Goussard to use the database of the parent study which is included as Appendix B.

Patient confidentiality was maintained by allocating study numbers and only the principle investigator had access to the codes.

3. Results

3.1. Demographics

The original database of patients included a total number of 212 patients, of which only 41 had a CXR available. Of those 41 patients only 37 had a CT MinIP and 4 did not, thus the final study population was 37 in total (Fig 3.1). The ages of the patients ranged from 2months 22 days to 147 months 25 days. The median age of the patients was 14.3 months (interquartile range 8.0-23.2 months; range 2.7-147.8 months). The total number of bronchi evaluated was calculated as follows: 37 patients x 10 sites = 370 bronchi (Fig 3.2).

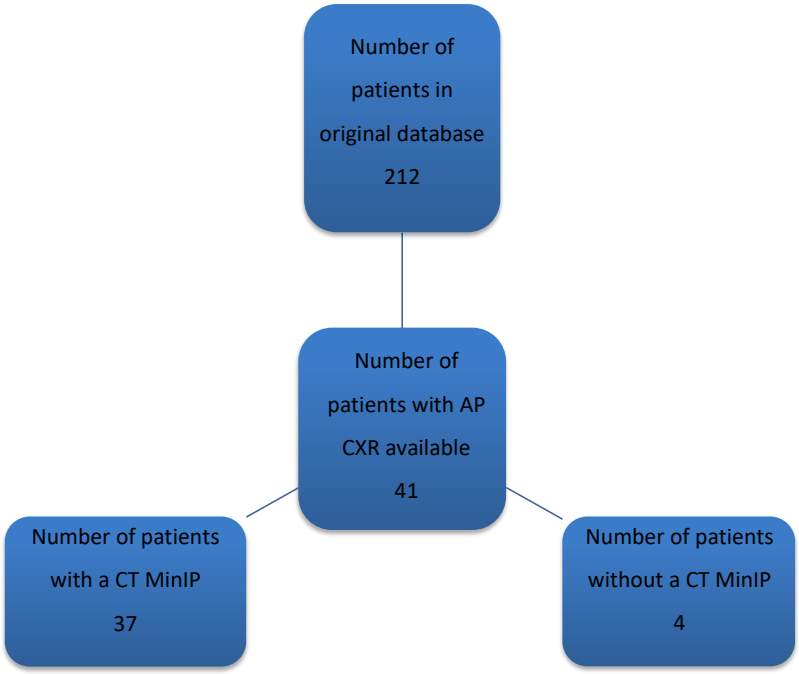

Figure 3.1. Flow diagram demonstrating the derivation of included patients

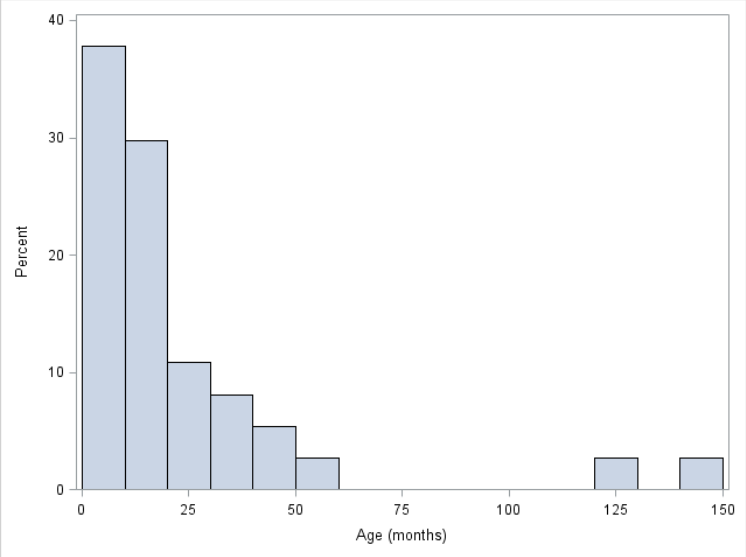

Figure 3.2. Age of patients (n = 37)

3.2. Presence of airway stenosis by site

Figure 3.3. and Table 3.1. demonstrate the percentage of patients with stenosis picked up by each modality according to airway site. The sites found to have the greatest percentage of patients with stenosis were the LMB and BI. At the LMB 83.9% of patients had stenosis on CXR and 89.2% had stenosis on CT MinIP. At the BI 72.4% of patients had stenosis on CXR and 89.2% had stenosis on CT MinIP.

Table 3.1. Percentage of patients with stenosis diagnosed by each modality

	CXR			MinIP		
Site	n	Number of patients with stenosis	Percentage of patients with stenosis	n	Number of patients with stenosis	Percentage of patients with stenosis
Trachea	31	5	16.1%	36	24	66.7%
Carina	29	3	10.3%	37	12	32.4%
RMB	28	5	17.9%	37	21	56.8%
RULB	16	2	12.5%	37	27	73%
BI	29	21	72.4%	37	33	89.2%
RMLB	16	7	43.8%	37	11	29.7%
RLLB	24	11	45.8%	37	7	18.9%
LMB	31	26	83.9%	37	33	89.2%
LULB	22	3	13.6%	37	22	59.5%
LLLB	25	7	28%	37	24	64.9%

*All the sites evaluated on the CXR shows a lower sample size n than the study population of 37, this is due to poor quality of the radiograph causing non visualization of the structure
**CT MinIP evaluation of the trachea shows a lower sample size of 36 due to poor quality of one MinIP causing non visualization of the structure

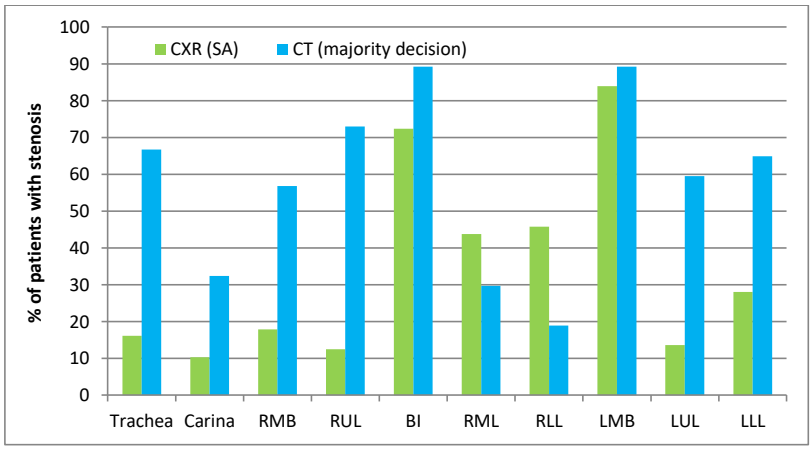

Figure 3.3. Percentage of stenosis by site as determined by CXR and CT MinIP

Table 3.2. demonstrates the sensitivity and the specificity of CXR for the detection of stenosis for each site. According to the table, the sensitivity of CXR for picking up stenosis at the LMB is the highest 92.9% with a lower confidence limit of more than 75%. It has a 100% specificity but the confidence interval is very wide. The sensitivity for picking up stenosis at the BI is the second highest, at 80% with a reasonable lower confidence limit of 59.3%. The specificity is 75% but has a very wide confidence interval. The RMLB and RLLB have a good sensitivity but due to a low sample size (n) the confidence intervals are wide. Thus the sensitivity for picking up stenosis on CXR is the highest at the LMB and the BI.

Table 3.2. Estimation of the sensitivity and specificity of CXR for the detection of stenosis against CT MinIP for each site

Site	Sensitivity (%)			Specificity (%)		
	n	Estimate	95% CI	n	Estimate	95% CI
Trachea	*21*	9.5	1.2-30.4	*10*	70.0	34.8-93.3
Carina	*10*	20.0	2.5-55.6	*19*	94.7	74.0-99.9
RMB	*17*	23.5	6.8-49.9	*11*	90.9	58.7-99.8
RULB	*11*	18.2	2.3-51.8	*5*	100.0	47.8-100.0
BI	*25*	80.0	59.3-93.2	*4*	75.0	19.4-99.4
RMLB	*6*	83.3	35.9-99.6	*10*	80.0	44.4-97.5
RLLB	*5*	80.0	28.4-99.5	*19*	63.2	38.4-83.7
LMB	*28*	92.9	76.5-99.1	*3*	100.0	29.2-100.0
LULB	*16*	18.8	4.1-45.7	*6*	100.0	54.1-100.0
LLLB	*17*	41.2	18.4-67.2	*8*	100.0	63.1-100.0

3.3. Severity of stenosis on CXR and MinIP

3.3.1. By site

The percentage of severe stenosis at a site was calculated as follows: Percentage severe stenosis at site = severe stenosis at site ÷ total number of stenoses (all grades and sites). Severe stenosis was taken as grade 3a and 3b. The grading scale used is summarised in the methods section.

Figure 3.4. and Table 3.3. summarise the percentage of severe stenosis at a site according to CXR and demonstrate that the highest total number of stenoses for a site, all grades combined (1+2+3a+3B) were identified at the LMB (25) and BI (20). The highest number of severe stenoses (grade 3a +3b) for a site was identified at the BI (9) and LMB (6). The total number of stenoses identified by CXR, all grades and all sites combined, totalled 83. On CXR the highest percentage of severe stenoses out of the total number of stenoses was picked up at BI (11%), LMB (7%) and RLLB (7%).

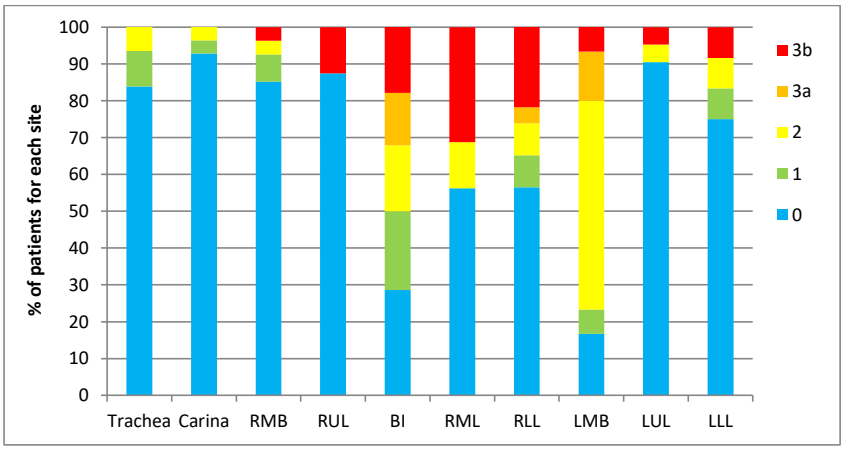

Figure 3.4. Grading of stenosis on CXR

Table 3.3. Percentage of severe stenosis per site according to CXR evaluation

CXR								
Site	Number of stenoses at site according to Grade Gr 1 2 3a 3b					Total number of stenoses at site *	Total number of severe stenoses at site **	% of severe stenosis at site ***
TRACHEA		3	2	0	0	5	0	
CARINA		1	1	0	0	2	0	
RMB		2	1	0	1	4	1	1/83x100= 1%
RULB		0	0	0	2	2	2	2/83x100= 2%
BI		6	5	4	5	20	9	9/83x100= 11%
RMLB		0	2	0	5	7	5	5/83x100= 6%
RLLB		2	2	1	5	10	6	6/83x100= 7%
LMB		2	17	4	2	25	6	6/83x100= 7%
LULB		0	1	0	1	2	1	1/83x100= 1%
LLLB		2	2	0	2	6	2	2/83x100= 2%
TOTAL		18	33	9	23	83	32	32/83x100= 39%

***Grade 1+2+3a+3b**
**** Grade 3a + 3b**
***** Total Severe stenoses at site = (3a + 3b)÷total number of stenoses (83)**

Evaluating figure 3.5. and table 3.4. for the percentage of severe stenosis at a site according to CT MinIP demonstrates that the highest total number of stenoses for all sites, all grades combined (1+2+3a+3B) was present at the LMB (34) and BI (33). The highest number of severe stenoses (grade 3a +3b) for a site was present at the LMB (16) and the BI (14). The total number of stenoses identified by CT MinIP, all grades and all sites combined, was 214. On CT MinIP the highest percentage of severe stenosis out of the total number of stenoses was present at the LMB (7%) and BI (7%).

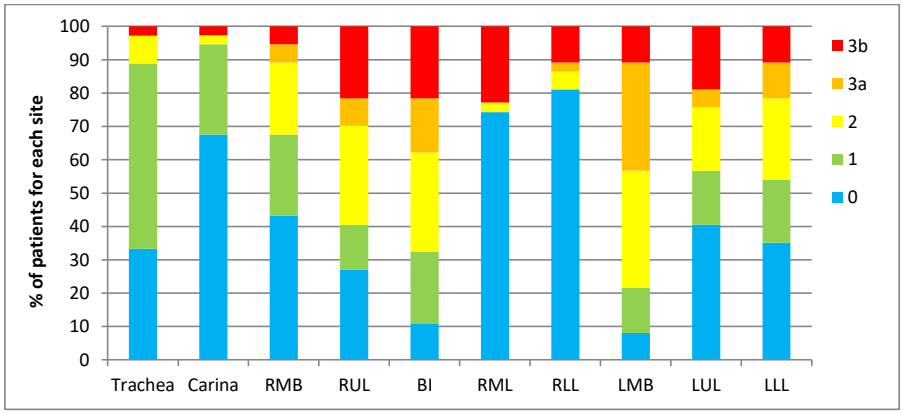

Figure 3.5. Grading of stenosis on CT

Table 3.4. Percentage of severe stenosis per site according to CT MinIP evaluation

CT MinIP								
Site	Number of stenoses at site according to Grade Gr 1	2	3a	3b	Total number of stenoses at site*	Total number of severe stenoses at site**	% of severe stenosis at site ***
TRACHEA	20	3	0	1	24	1	1/214X100= 0%
CARINA	10	1	0	1	12	1	1/214X100= 0%
RMB	9	8	2	2	21	4	4/214X100= 2%
RULB	5	11	3	8	27	11	11/214X100= 5%
BI	8	11	6	8	33	14	14/214X100= 7%
RMLB	0	1	0	9	10	9	9/214X100= 4%
RLLB	0	2	1	4	7	5	5/214X100= 2%
LMB	5	13	12	4	34	16	16/214X100= 7%
LULB	6	7	2	7	22	9	9/214X100= 4%
LLLB	7	9	4	4	24	8	8/214X100= 4%
Total	70	66	30	48	214	78	78/214x100= 36%

***Grade 1+2+3a+3b**
**** Grade 3a + 3b**
***** Total Severe stenoses at site (3a + 3b) ÷ total number of stenoses (214)**

Evaluating Table 3.5. for the kappa agreement between CXR and CT MinIP with regards to the grade of stenosis for each site shows that the highest weighted kappa agreement between the modalities was at the LMB, substantial agreement (Kappa 0.67) and BI, moderate agreement (kappa 0.58)

Table 3.5. Agreement between CXR and CT MinIP with regards to the grade of obstruction for each site

Site	Agreement		
	n	weighted κ	interpretation
Trachea	*31*	0.30	fair agreement
Carina	*28*	0.51	moderate agreement
RMB	*27*	0.10	slight agreement
RULB	*16*	0.34	fair agreement
BI	*28*	0.58	moderate agreement
RMLB	*16*	0.57	moderate agreement
RLLB	*23*	0.35	fair agreement
LMB	*30*	0.67	substantial agreement
LULB	*21*	0.22	fair agreement
LLLB	*24*	0.25	fair agreement

Commented [DB1]:

3.3.2. Overall number of stenoses according to severity for CXR and CT MinIP

Table 3.7. demonstrates that CXR picked up grade 3a stenosis 9 times and grade 3b stenosis 23 times, totalling of 32 severe stenoses picked up. CT MinIP demonstrated grade 3a stenosis 30 times and 3b stenosis 48 times, totalling 78 severe stenosis picked up.

Table 3.6. Overall number of stenosis according to severity for CXR and CT MinIP

Severity (proportion of occlusion)	CXR	CT MinIP
3a (76-99%)	9	30
3b (100%)	23	48
Total severe stenosis	32	78

3.3.3. Number of patients who demonstrated stenosis in any of the ten predetermined sites

Chest X-ray demonstrated that 31 out of the 37 patients in the study group thus 84%, had stenosis at least at one of the ten evaluated sites, confirmed on the CT MinIP images. Computed tomography MinIP, which is taken as the gold standard, showed that all 37 patients, thus 100%, had stenosis at one of the ten evaluated sites.

4. Discussion

Tuberculosis is an infection caused by the bacteria *M. tuberculosis* (1). Inhalation of *M. tuberculosis* bacilli is the most frequent mode of infection. Inhalation of an infectious droplet is the start of the infective process with the pathogen lodging in a terminal airway or alveoli causing a localised lung response described as the primary parenchymal or Ghon focus (9). Tuberculosis bacilli drain away from this focus through the local lymphatic pathways to the regional lymph nodes (9). These lymph nodes may enlarge by becoming oedematous and hyperaemic with the formation of tuberculous cavitating granulomas and areas of caseation (5). Lymphobronchial tuberculosis occurs when tuberculous lymphadenopathy compresses and infiltrates the adjacent airway wall, causing extra- or intra-luminal airway obstruction (35). Children younger than 5 years old are especially prone to this phenomenon of airway involvement as their airways are small (35) and also more compressible and pliable (39). In this regard, we note that the median age of the patients included in our study was 14.3 months, which was lower than the age distribution in studies by Maydell et al (20 months) (34), and du Plessis and colleagues (21 months) (24). It is often very challenging to prove the diagnosis of TB in paediatric patients due to the fact that this organism is cultured in only a small number of cases (27, 40, 41), thus the diagnosis of primary TB in children relies to a great extent on the visualisation of mediastinal lymphadenopathy on radiographs (33).

Various modalities are available to evaluate the paediatric airway but the pros and cons of each must be carefully weighed up. One of the important considerations is the fact that paediatric patients are more susceptible to radiation from radiological procedures due to their organs which are not yet mature and still developing, their short stature causing sensitive organs to be situated closely together, and longer lifespan in which to develop malignancies (42), thus it has to be taken into consideration that the patient is exposed to additional radiation when a CT is done (26).

The radiation dose of a chest radiograph is relatively low compared to CT scanning (42) therefore AP and lateral CXR is the first and the most frequently used radiological

modality in children (1). It has previously been reported that approximately 60 % of patients with a normal CXR will demonstrate lymphadenopathy on a chest CT (24), thus this method is insensitive for the detection of lymphadenopathy (13, 24). An AP CXR may however be used in children to evaluate for airway displacement and constriction as an indirect sign of lymphadenopathy (31). Compression of either of the main bronchi is an indirect sign of subcarinal lymph node enlargement (35). Chest X-ray is also useful for depicting airspace disease, the Ghon focus, interstitial disease and pleural effusions (13). There is marked interobserver variability amongst paediatric radiologists when chest radiographs are evaluated for lymphadenopathy (43). We encountered the same interobserver variability in our study with the reading of CXR by three radiologists, thus we chose to use the results of the expert reader to eliminate variability.

Computed tomography MinIP is an exceptionally effective visualisation technique for evaluation of the large airways (36, 37) especially in children (38). Anatomical structures that are not orientated in a single plane can be evaluated in their entirety (37), thus the length of airway strictures can be seen on one slice (26). Computed tomography is the preferred method of investigation for lymph node detection in the chest (33), it is not difficult to perform and no anaesthesia is needed due to the quick acquisition of images. The need for IV contrast media for distinguishing lymphadenopathy from vessels is however a limitation (13). Availability of CT and radiological services in general are poor in developing countries due to poor infrastructure, poor support and maintenance services as well as a shortage of health professionals (44). This was demonstrated by Shimelis and colleagues in Addis Ababa, Ethiopia with only 18% CT scan availability (44).

Another useful technique used by many authors, is FTB, which is used to confirm airway stenosis, to evaluate the amount of narrowing, remove endobronchial material and to do a transbronchial biopsy. The procedure is safe if performed by a competent operator but has the disadvantages of being invasive, the need for general anaesthesia and may have ramifications such as subglottic oedema, hypercarbia, hypoxaemia and cardiac arrhythmia. The procedure also has the disadvantages of not being able to demonstrate the reason for stenosis and relationship with adjacent structures as well as navigating airways beyond severe stenosis (24).

The aim of the current study however was not to show which method for determining stenosis is the best, as we already know that CT MinIP and bronchoscopy outperforms CXR, but it is to prove that CXR, which is a low cost and easily available modality, can be sensitive and specific for picking up airway stenosis as a surrogate for lymphadenopathy in diagnosing TB in children, in a resource constrained environment. We demonstrated that the LMB and the BI were the commonest sites for stenosis on CXR as well as when using the gold standard CT MinIP. These findings compared well to research by other authors on the commonest site of stenosis including: Richter-Joubert et al, LMB and BI (45); Maydel et al BI, LMB (34); and Du Plessis et al BI, LMB (24). According to a study by Andronikou et al the most prevalent sites for TB lymph node enlargement were found to be subcarinal (90%), right hilar (74%), left hilar (72%) and bilateral hilar (61%), with the subcarinal group of nodes being the largest (33). The longer and narrower nature of the LMB in comparison to the RMB is the likely cause for the LMB more commonly occluded than the RMB (11, 33). It is postulated by Lucas et al that the compression of the BI is due to the location between two major involved lymph node groups, the subcarinal and right hilar groups, due to a "nutcracker" phenomenon (11).

Our study showed that the AP chest radiograph has a high sensitivity and specificity for picking up stenosis, especially at LMB and BI in our patient population. Because we used CT MinIP as a gold standard we had a smaller sample size, but this gold standard meant that our findings were significant despite this smaller sample size. Our patient population constituted children with LBTB and therefore all had clinical evidence of airway stenosis. We have shown that the demonstration of airway stenosis on CXR in these patients could be sufficient for the diagnosis, and that these patients do not require further investigation to confirm the airway involvement because of the sensitivity and specificity of the CXR.

Richter-Joubert et al also looked at the presence of airway stenosis in children with suspected TB, but did not have CT MinIP as a gold standard (45). Although this was a larger sample size, the study cannot comment on sensitivity and specificity of these findings in the absence of a gold standard. Instead, they used majority decision of three

readers to decide on the presence of a stenosis against the final diagnosis based on laboratory testing. They also found that the commonest site of stenosis is the BI and LMB.

Our study found that severe stenosis (76-100%) was commonest at the LMB, BI and RLLB on CXR, and LMB, BI on CT MinIP imaging. Our findings correlate with other authors such as Goussard et al who also describe the BI as a common region for complete airway obstruction (35). Our findings differ from a study by Du Plessis who found the commonest site of severe compression to be the RULB (24). Figure 3.4 gives a misleading high estimation of the severe stenosis (3a and 3b) encountered on CXR at the RMLB and RLL bronchi (this is again due to non-visualisation of the airway by our expert reader either due to true stenosis or technical factors) and adds to our studies limitations. As the subcarinal group of lymph nodes was found by other authors to be the most frequently involved (13, 33), and also the position of the most substantial lymph node mass in the greatest number of patients (33), the close relationship of the LMB and BI to this enlarged lymph node group may be one of the reasons why the most severe compression occurred at these sites. In our study we demonstrated that the kappa agreement between CXR and MinIP for the grade of stenosis was the greatest at the LMB (substantial agreement Kappa 0.67) and BI (moderate agreement Kappa 0.58). Our study demonstrated that CT MinIP outperformed AP CXR when evaluating for airway narrowing by demonstrating 214 stenoses and 78 severe stenoses versus 83 stenoses and 32 severe stenoses found by CXR. However, CXR demonstrated that 31 out of the 37 patients (84%), had stenosis at least at one of the ten evaluated sites, confirmed on the goldstandard CT MinIP images. Computed tomography MinIP showed that all 37 patients (100%) had stenosis at least at one of the ten evaluated sites but this is expected since the study population is a subgroup of patients who had airway symptoms and confirmed TB which qualified them for the CT scan in the clinical setting. Our results of CT MinIP superiority over plain radiographs are not surprizing as the general advantages of CT over chest radiographs in depicting the degree of tuberculous disease and the complications thereof, have been well documented (46). We therefore used the CT scan MinIP as a gold standard for determining specificity and sensitivity.

4.1. Limitations of the current study

The sample size of this study was small, because only patients that had both CT MinIP and CXR available for evaluation were included in the study. Although the presence of a gold standard (CT MinIP) enabled us to demonstrate high sensitivity and specificity, the small sample size resulted in wide confidence intervals.

The study population was biased as all the children had airway compression symptoms thus there was a preselected population of children, however not all airways are involved in all children, therefore this provided an adequate population for comparing the presence of airway stenosis. It is also not ethical to perform CT scans in normal children to serve as controls.

In a number of CXR cases it was not possible to evaluate all the airways and on one CT MinIP image the trachea, as they were not visualised due to technical factors. As a result on all the CXR's and one CT MinIP the sample size n at the different sites is less than the study population of 37.

The frontal radiographs were interpreted by all three readers separately, the interpretations of SA were however used as those of the expert reader because of marked interobserver differences, and compared to the CT MinIP images.

Between the interpretation of the CXR and CT MinIP images some months were given to allow for a washout period, there is however always the potential for recall bias.

4.2. Current applications

CXR can thus be used to diagnose stenosis at the LMB and BI in children younger than 2 years of age in a population where the incidence and severity of stenosis is high, but also in populations where the incidence of airway symptoms are low in the following circumstances: While the clinician is awaiting a confirmatory diagnosis of TB or when no diagnosis is available, and importantly when the hilum is hidden by airspace disease, in patients where the heart or thymus shadow obscures the hila, where there is disagreement on the presence of soft tissue lymph node masses and where CT and MRI are not available.

4.3. Future applications

Work to be done in a future study may include a prospective study with a larger patient base, with more than one reader in a population where the incidence and severity of airway

stenosis is lower, the caveat being that no gold standard such as CT or bronchoscopy will likely be available in this setting.

5. Conclusion

The diagnosis of TB and especially LBTB relies heavily on imaging to demonstrate airway compression due to enlarged lymph nodes. In the paediatric population where the incidence and the severity of stenosis is high, CXR was shown to have a good sensitivity and specificity for detecting stenosis and had a good agreement with CT MinIP as gold standard in demonstrating severe grade of stenosis at the LMB and BI. In children with clinical symptoms of airway compression and suspected TB, airway stenosis involving the LMB and BI on CXR can be considered a surrogate for the presence of lymphadenopathy and is useful for making the diagnosis of TB.

In countries with resource constraints and a high burden of disease this cheap and effective imaging modality may assist in the early diagnosis and treatment of TB, which in turn may assist the WHO global TB program and the end TB strategy to achieve their goal of ending the global TB epidemic.

6. References

(1) Lucaya J, Strife JL, Baert AL. Ch. 7. In: Pediatric chest imaging: Chest imaging in infants and children Softcover reprint of hardcover 2nd ed. 2008 ed ed.: Springer; Softcover reprint of hardcover 2nd ed. 2008 edition (May 15, 2011), 2008, p. 165-81.

(2) Cremin BJ, Jamieson DH. Ch. In: Childhood tuberculosis: modern imaging and clinical concepts, ed. Berlin Heidelberg New York: Springer; Softcover reprint of the original 1st ed. 1995 edition (December 16, 2011, 1995, p. 19-50.

(3) Raviglione MC. 2003. The TB epidemic from 1992 to 2002. *Tuberculosis (Edinb)*, 83(1-3):4-14.

(4) Organization WH. Global tuberculosis report 2016 http://www.who.int/tb/publications/global_report/en/.

(5) Buxi TB, Sud S, Vohra R. 2002. CT and MRI in the diagnosis of tuberculosis. *Indian J Pediatr*, 69(11):965-72.

(6) Organization WH. Global tuberculosis report 2013 http://www.who.int/iris/handle/10665/91355.

(7) Massyn NP, N.; English, R.; Padarath, A.; Barron, P.; Day, C. District Health Barometer 2015/2016. Durban: Health Systems Trust; 2016. p. 180 - 208.

(8) Cohen J. Reversal of Misfortunes. science. 2013 22 February.

(9) Marais BJ, Gie RP, Schaaf HS, *et al.* 2004. A proposed radiological classification of childhood intra-thoracic tuberculosis. *Pediatr Radiol*, 34(11):886-94.

(10) De Villiers RV, Andronikou S, Van de Westhuizen S. 2004. Specificity and sensitivity of chest radiographs in the diagnosis of paediatric pulmonary tuberculosis and the value of additional high-kilovolt radiographs. *Australas Radiol*, 48(2):148-53.

(11) Lucas S, Andronikou S, Goussard P, *et al.* 2012. CT features of lymphobronchial tuberculosis in children, including complications and associated abnormalities. *Pediatr Radiol*, 42(8):923-31.

(12) Papagiannopoulos KA, Linegar AG, Harris DG, *et al.* 1999. Surgical management of airway obstruction in primary tuberculosis in children. *Ann Thorac Surg*, 68(4):1182-6.

(13) Andronikou S, Wieselthaler N. 2004. Modern imaging of tuberculosis in children: thoracic, central nervous system and abdominal tuberculosis. *Pediatr Radiol*, 34(11):861-75.

(14) Marais BJ, Gie RP, Schaaf HS, *et al.* 2006. Childhood pulmonary tuberculosis: old wisdom and new challenges. *Am J Respir Crit Care Med*, 173(10):1078-90.

(15) Marais BJ, Hesseling AC, Gie RP, *et al.* 2006. The bacteriologic yield in children with intrathoracic tuberculosis. *Clin Infect Dis*, 42(8):e69-71.

(16) Weismuller MM, Graham SM, Claessens NJ, *et al.* 2002. Diagnosis of childhood tuberculosis in Malawi: an audit of hospital practice. *Int J Tuberc Lung Dis*, 6(5):432-8.

(17) Walls T, Shingadia D. 2004. Global epidemiology of paediatric tuberculosis. *J Infect*, 48(1):13-22.

(18) Cuevas LE, Petrucci R, Swaminathan S. 2012. Tuberculosis diagnostics for children in high- burden countries: what is available and what is needed. *Paediatrics and International Child Health*, 32(2):7.

(19) Kashif RU, Faizan M, Anwar S. 2019. Pediatric Malignant Mediastinal Masses. *J Coll Physicians Surg Pak*, 29(3):258-62.

(20) Parambil AS, Prem S, Jacob PM, *et al.* 2016. Mediastinal Mass with Hyper-eosinophilia in a Young Boy -A Diagnostic Dilemma. *J Clin Diagn Res*, 10(7):XD03-XD04.

(21) Bartram U, Thul J, Bauer J, *et al.* 2006. Systemic sarcoidosis after cardiac transplantation in a 9-year-old child. *J Heart Lung Transplant*, 25(10):1263-7.

(22) Becroft DM, Dix MR, Gillman JC, *et al.* 1973. Benign sinus histiocytosis with massive lymphadenopathy: transient immunological defects in a child with mediastinal involvement. *J Clin Pathol*, 26(7):463-9.

(23) Enarson PM, Enarson DA, Gie R. 2005. Management of tuberculosis in children in low-income countries. *Int J Tuberc Lung Dis*, 9(12):1299-304.

(24) du Plessis J, Goussard P, Andronikou S, *et al.* 2009. Comparing three-dimensional volume-rendered CT images with fibreoptic tracheobronchoscopy in the evaluation of airway compression caused by tuberculous lymphadenopathy in children. *Pediatr Radiol*, 39(7):694-702.

(25) Kim WS, Moon WK, Kim IO, *et al.* 1997. Pulmonary tuberculosis in children: evaluation with CT. *AJR Am J Roentgenol*, 168(4):1005-9.

(26) Andronikou S, Irving B, Hlabangana LT, *et al.* 2013. Technical developments in postprocessing of paediatric airway imaging. *Pediatr Radiol*, 43:16.

(27) Bosch-Marcet J, Serres-Creixams X, Zuasnabar-Cotro A, *et al.* 2004. Comparison of ultrasound with plain radiography and CT for the detection of mediastinal lymphadenopathy in children with tuberculosis. *Pediatr Radiol*, 34(11):895-900.

(28) Herth FJ, Becker HD. 2003. Transthoracic ultrasound. *Respiration*, 70(1):87-94.

(29) Beckh S, Bolcskei PL, Lessnau KD. 2002. Real-time chest ultrasonography: a comprehensive review for the pulmonologist. *Chest*, 122(5):1759-73.

(30) Leung AN, Muller NL, Pineda PR, *et al.* 1992. Primary tuberculosis in childhood: radiographic manifestations. *Radiology*, 182(1):87-91.

(31) Andronikou S, Vanhoenacker FM, De Backer AI. 2009. Advances in imaging chest tuberculosis: blurring of differences between children and adults. *Clin Chest Med*, 30(4):717-44, viii.

(32) Van Dyck P, Vanhoenacker FM, Van den Brande P, *et al.* 2003. Imaging of pulmonary tuberculosis. *Eur Radiol*, 13(8):1771-85.

(33) Andronikou S, Joseph E, Lucas S, *et al.* 2004. CT scanning for the detection of tuberculous mediastinal and hilar lymphadenopathy in children. *Pediatr Radiol*, 34(3):232-6.

(34) Maydell A, Goussard P, Andronikou S, *et al.* 2010. Radiological changes post-lymph node enucleation for airway obstruction in children with pulmonary tuberculosis. *Eur J Cardiothorac Surg*, 38(4):478-83.

(35) Goussard P, Gie R. 2007. Airway involvement in pulmonary tuberculosis. *Paediatr Respir Rev*, 8(2):118-23.

(36) Rubin GD. 2003. 3-D imaging with MDCT. *Eur J Radiol*, 45 Suppl 1:S37-41.

(37) Kirchgeorg MA, Prokop M. 1998. Increasing spiral CT benefits with postprocessing applications. *Eur J Radiol*, 28(1):39-54.

(38) Perandini S, Faccioli N, Zaccarella A, *et al.* 2010. The diagnostic contribution of CT volumetric rendering techniques in routine practice. *Indian J Radiol Imaging*, 20(2):92-7.

(39) Goussard P, Gie RP, Kling S, *et al.* 2012. Bronchoscopic assessment of airway involvement in children presenting with clinically significant airway obstruction due to tuberculosis. *Pediatr Pulmonol*.

(40) Vallejo JG, Ong LT, Starke JR. 1994. Clinical features, diagnosis, and treatment of tuberculosis in infants. *Pediatrics*, 94(1):1-7.

(41) [No authors listed]. 1990. American Thoracic Society. Diagnostic standards and classification of tuberculosis. *Am Rev Respir Dis*, 142(3):725-35.

(42) Andronikou S, Fink AM. 2002. Radiation risk in paediatric CT. *S Afr Med J*, 92(7):516.

(43) Du Toit G, Swingler G, Iloni K. 2002. Observer variation in detecting lymphadenopathy on chest radiography. *Int J Tuberc Lung Dis*, 6(9):814-7.

(44) Shimelis D, Atnafu A. 2011. Status of radiological services in Addis Ababa public hospitals. *Ethiop Med J*, 49(3):257-63.

(45) Richter-Joubert L, Andronikou S, Workman L, *et al.* 2017. Assessment of airway compression on chest radiographs in children with pulmonary tuberculosis. *Pediatr Radiol*.

(46) Choe KO, Jeong HJ, Sohn HY. 1990. Tuberculous bronchial stenosis: CT findings in 28 cases. *AJR Am J Roentgenol*, 155(5):971-6.

Appendix A: Ethics Clearance Certificate

R14/49 Dr Dewald Bester et al

HUMAN RESEARCH ETHICS COMMITTEE (MEDICAL)

CLEARANCE CERTIFICATE NO. M140476

NAME: (Principal Investigator)	Dr Dewald Bester et al
DEPARTMENT:	Radiology Tygerberg Hospital, Paroe, Western Cape
PROJECT TITLE:	Comparison of X-Ray and Coronal Minimum Intensity Projection Computed Tomography Findings of Airway Compression from Lymphobroncial Tuberculosis in Children
DATE CONSIDERED:	25/04/2014
DECISION:	Approved unconditionally
CONDITIONS:	
SUPERVISOR:	Dr Susan Lucas
APPROVED BY:	Professor PE Cleaton-Jones, Chairperson, HREC (Medical)
DATE OF APPROVAL:	29/04/2014

This clearance certificate is valid for 5 years from date of approval. Extension may be applied for.

DECLARATION OF INVESTIGATORS

To be completed in duplicate and **ONE COPY** returned to the Secretary in Room 10004, 10th floor, Senate House, University.

I/we fully understand the conditions under which I am/we are authorized to carry out the above-mentioned research and I/we undertake to ensure compliance with these conditions. Should any departure be contemplated, from the research protocol as approved, I/we undertake to resubmit the application to the Committee. **I agree to submit a yearly progress report**.

Principal Investigator Signature — Date 1/5/2014

PLEASE QUOTE THE PROTOCOL NUMBER IN ALL ENQUIRIES

Appendix B: Permission letter from Prof P. Goussard

UNIVERSITEIT · iYUNIVESITHI · STELLENBOSCH · UNIVERSITY

100
1918 · 2018

30 January 2020

The Chair
The Institutional Review Board
Faculty of Health Sciences
University of the Witwatersrand

Dear Chair

PERMISSION FOR DR DEWALD BESTER

The letter dated 5 March 2013 provided by Prof RP Gie refers. In the letter, Dr Dewald Bester was wrongly referred to as "Dr Botha".

We herewith therefore confirm:

Dr Bester is working with Dr Su Lucas in a collaborative study with the Department of Paediatrics and Child Health, Stellenbosch University.

The project is on comparing reconstructed computer tomography images with chest radiographs to determine airway narrowing cause by Mycobacterium tuberculosis in children. The data for the study was collected by Prof RP Gie and myself and is part of ongoing research. The research has been approved by the Human Research Committee of the Faculty of Medicine and Health Sciences, Stellenbosch University. All the studies were done with the informed consent of the parents or legal guardians.

Kind regards

PROF PIERRE GOUSSARD
Head of Clinical Unit: Paediatric Pulmonology and Paediatric Intensive Care
Department of Paediatrics and Child Health, Stellenbosch University and Tygerberg Hospital

Departement Pediatrie en Kindergesondheid / Department of Paediatrics and Child Health
Faculty of Medicine and Health Sciences | Fakulteit Geneeskunde en Gesondheidswetenskappe
P O Box 241, Posbus 241, Cape Town, Kaapstad, 8000 |
Tel: +27 21 938 9506 | E-pos / Email: pgouss@sun.ac.za | http://www.sun.ac.za/english/faculty/healthsciences/

Appendix C: Tick sheet site and degree of airway narrowing on CXR

Site and degree of airway narrowing on CXR

Study number: _____ Age: _____

Grade of obstruction	
0 = No Obstruction	0 %
1 = Mild Obstruction	1 - 50 %
2 = Moderate Obstruction	51 – 75 %
3a = Severe Obstruction	76 – 99 %
3b = Total obstruction	100 %

	Stenosed	Airway Measurements		Calculations	
Site	Y/N	Normal calibre of airway above stenosis N	Maximum Stenosis S	% attenuation = 1- S/N x 100	Grade
Trachea					
Carina					
RMB					
RUL					
BI					
RML					
RLL					
LMB					
LUL					
LLL					

Appendix D: Tick sheet site and degree of airway narrowing on CT MinIP

Site and degree of airway narrowing on MinIP

Study number: _____ Age: _____

Grade of obstruction	
0 = No Obstruction	0 %
1 = Mild Obstruction	1 - 50 %
2 = Moderate Obstruction	51– 75 %
3a = Severe Obstruction	76 – 99 %
3b = Total obstruction	100 %

	Stenosed	Airway Measurements		Calculations	
Site	Y/N	Normal calibre of airway above stenosis N	Maximum Stenosis S	% attenuation = S/N x 100	Grade
Trachea					
Carina					
RMB					
RUL					
BI					
RML					
RLL					
LMB					
LUL					
LLL					

Appendix E: Note on referencing style

Please note that the referencing in this thesis is a modification of the Vancouver Referencing style, done according to the Faculty of Health Sciences Style Guide as set out by the Wits Health Sciences Library.

The information on this WHSL Vancouver Citation Style Guide for Theses, Dissertations and Research Reports is available from http://libguides.wits.ac.za/whsl-vancouver updated on 30 January 2017.